Korean J. Chem. Eng., 33(5), 1706-1711 (2016)
DOI: 10.1007/s11814-015-0291-8

pISSN: 0256-1115
eISSN: 1975-7220

Tuning magnetism via selective injection into ice-like clathrate hydrates

Youngjune Park*,†, Dong-Yeun Koh, Joonghoe Dho***, Sun-Hwa Yeon****, and Huen Lee*****,†**

*School of Environmental Science and Engineering, Gwangju Institute of Science and Technology (GIST), 123, Cheomdangwagi-ro, Buk-gu, Gwangju 61005, Korea
**School of Chemical & Biomolecular Engineering, Georgia Institute of Technology, 311 Ferst Drive NW, Atlanta, Georgia 30332-0100, U.S.A.
***Department of Physics, Kyungpook National University, Daegu 41566, Korea
****Korea Institute of Energy Research, 152, Gajeong-ro, Yeseong-gu, Daejeon 34129, Korea
*****Department of Chemical and Biomolecular Engineering (BK21+ Program), Korea Advanced Institute of Science and Technology, 291, Daehak-ro, Yuseong-gu, Daejeon 34141, Korea
(*Received 31 October 2015 • accepted 18 December 2015*)

Abstract−Clathrate hydrates exhibit unique intermolecular interactions between host-guest and guest-guest molecules because they have 3-dimensional superstructures consisting of the sublattices created by hydrogen-bonded water molecules that form cage-like frameworks in which guest molecules can be incorporated. Lattice engineering or molecular engineering using a selective injection of specific guest molecules into these sublattices can be exploited to tune the physicochemical properties of guest molecules or to create new functional materials. Here, we report distinctive intermolecular behavior of oxygen molecules that are selectively inserted in a structure-II type superstructure consisting of a tetrahedral sublattice by the small 5^{12} water cages and a diamond-like sublattice by the large $5^{12}6^4$ cages. Pure O_2 clathrate hydrate and binary THF+O_2 clathrate hydrate were synthesized, and their magnetism and heat capacity were measured at low temperature conditions. These results strongly suggest that the magnetic property of the oxygen molecule is largely varied with the formation of a 3-dimensional superstructure by the injection of O_2 into the water frameworks.

Keywords: Clathrate, Gas Hydrate, Oxygen, Magnetism, Tetrahydrofuran

INTRODUCTION

In 1952, Pauling and Marsh proposed chlorine enclosed clathrate hydrate structures, *Pm3n*, with cell dimensions of 12 Å [1]. In common with water-ice, which is tetrahedrally coordinated four oxides, with two near covalently bonded protons and two far hydrogen-bonded protons, clathrate 'ice-like' structures are constructed by tetrahedrally coordinated oxygen atoms. As a 'host' lattice, crystallized water molecules offer polyhedral frameworks, so-called 'water-ice' cages, that can physically enclose other molecules, referred to as 'guests'. To be stacked regularly, those polyhedra must share each face as well as every vertex with neighboring polyhedra. However, the diameters of the polyhedra are typically larger than the van der Waals diameter of the non hydrogen-bonded oxygen atoms, and consequently the clathrate hydrate structure does not exist independently without occupation of guest molecules in water-ice cages [2].

Among the three well-known kinds of clathrate hydrate structures, structure-I (*sI*, cubic, *Pm3n*), structure-II (*sII*, cubic, *Fd3m*), and structure-H (*sH*, hexagonal, *P6/mmm*), the *sII* type clathrate hydrate is shown in Fig. 1(a). In the *sII* clathrate hydrate, its ideal unit cell consists of $16S{\cdot}8L{\cdot}136H_2O$, where the small 5^{12} (*S*, pentagonal dodecahedron) and large $5^{12}6^4$ (*L*, hexakaidecahedron) cages can be occupied by gaseous as well as liquid guest molecules [3]. Recently, the clathrate hydrate has attracted much attention as a safe storage material for energy gases [4] and as an unconventional natural gas for potential energy resources [5]. The *sII-L* and *sII-S* cages in the clathrate hydrate matrix are enclosed by water-ice. These cages with diameter 6-9 Å are regularly ordered and sufficiently to capture guest molecules or atomic clusters.

The guest molecules filled in *sII-S* and *sII-L* cages form a 3-dimensional (3-d) superstructure with two sublattices, *i.e.*, a tetrahedral sublattice by the *sII-S* cages and a diamond-like sublattice by the *sII-L* cages [6]. Therefore, various superstructural systems based on the clathrate hydrates can be synthesized by controlling the insertion of guest molecules with various physical properties into the water-ice cages. This technology may be exploited in lattice engineering or molecular engineering to change the physical properties of the guest system or to manufacture novel functional materials.

On the other hand, related to the tetrahedrally hydrogen-bonded water-ice structure, water-ice is a well-defined frustrated system, revealing that not all of the pair interactions can be minimized simultaneously because of local geometric constraints [7]. Pauling showed that the so-called 'ice-rule', where each oxide has two near and two far protons, as shown in Fig. 1(b), and does not make a regular arrangement of protons, but instead it gives rise to a degeneracy because such a 'two-in' and 'two-out' displacement of protons

†To whom correspondence should be addressed.
E-mail: young@gist.ac.kr, hlee@kaist.ac.kr
‡This article is dedicated to Prof. Huen Lee on the occasion of his retirement from KAIST.
Copyright by The Korean Institute of Chemical Engineers.

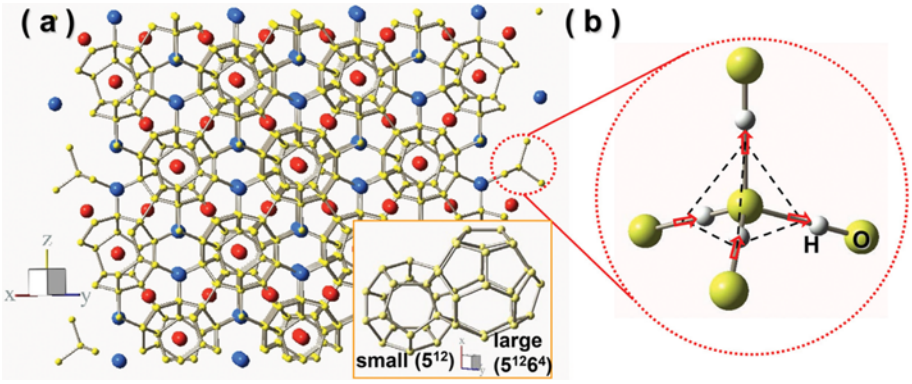

Fig. 1. Structures of clathrate hydrate. (a) Lattice structure of *sII* clathrate hydrate (16*S*·8*L*·136H_2O) with *sII-S* and *sII-L* cages where the guest molecules of THF and/or O_2 are stably enclosed. The *sII-L* cages can occupy both THF and O_2 molecules (blue balls), while the *sII-S* cages occupy only O_2 molecules (orange balls). The inset shows the water-ice framework structures of *sII-S* and *sII-L* cages where oxygen atoms in water framework are represented by yellow balls and protons were omitted for simplicity. (b) Oxygen-proton arrangement in water-ice satisfying the "ice-rule", *i.e.*, a 'two-in-two-out' configuration in the proton displacement. The open arrows represent the displacement vectors of protons (white ball).

has a diversity of energetically equivalent proton arrangements [8]. Quite interestingly, the frustration phenomenon realized in water-ice has been also observed in magnetic systems with certain lattice symmetries such as trigular or tetrahedral types [9-14]. Further, the recent 'spin-ice' discovery in frustrated magnetic pyrochlore materials has actively stimulated related research on this unique condensed matter physics, where the arrangement of four spins located on the corner of tetrahedra has a degeneracy similar to that of water-ice as a result of all the pair magnetic interactions [8,9,12-14]. Therefore, one can expect that a magnetic superstructure with two magnetic sublattices, as in typical antiferromagnetic materials or with the pyrochlore lattice similar to the well-known spin-ice materials, can be created by controlled occupation of magnetic molecules in the *sII-S* and *sII-L* cages.

Here, we have synthesized a binary THF+O_2 clathrate hydrate with magnetic O_2 molecules in small cages and non-magnetic THF molecules in large cages as well as a pure O_2 clathrate hydrate with magnetic O_2 molecules in both small and large cages, and their magnetisms and heat capacities were measured at low temperature conditions.

MATERIALS AND METHODS

1. Materials Preparation and Measurements

O_2, H_2, D_2, N_2, and CO_2 gas with a purity of 99.999 mol% used for the present study were supplied by Special Gas Co. (Korea). Tetrahydrofuran (THF, 99%) was purchased from Sigma-Aldrich Inc. (USA). Water with ultrahigh purity was supplied by Merck (Germany). The THF solution (5.56 mol% THF) for THF+gas hydrates and pure water for O_2 hydrate were frozen at 243 K for at least 1 day. The frozen sample was then ground into a fine powder (~120 μm) under liquid nitrogen. The fine power of 5.56 mol% THF solution and pure water was then placed in a high pressure vessel with 150 cm^3 internal volume. The fine particles of the 5.56 mol% THF solution were directly exposed to O_2, H_2, D_2, N_2, and CO_2 gas, respectively. The fine particles of pure water were also exposed to O_2 gas for the synthesis of a pure O_2 hydrate. Each gas except CO_2 was introduced into the vessel while maintaining 120 bar and 268 K for a week for complete conversion to the solid hydrates. The THF+CO_2 hydrate was synthesized under 30 bar and 273 K for a week. When the clathrate hydrates were completely converted, residual gases were promptly vented under a liquid nitrogen atmosphere. Subsequently, the powder samples were then packed into a quartz tube. For the magnetism measurements, the samples in the quartz tubes were then mounted on a Quantum Design Inc. (USA) Magnetic Property Measurement System (MPMS) at 150 K to prevent dissociation. Specific heat capacities of the binary THF+O_2 hydrate and pure O_2 hydrate were measured by a Physical Property Measurement System (PPMS, Quantum Design Inc.) equipped with the relaxation calorimeter accessary. A small piece of the THF+O_2 or pure O_2 hydrate sample (~5 mg) was mounted on a calorimeter puck under liquid nitrogen condition to prevent dissociation. Coupling (%) was also measured, which indicates how well or how poorly the sample is thermally attached to the sample holder. In general, sample coupling of less than 90% indicates poor contact. However, we aimed to measure the heat capacity for only a qualitative analysis because of the low coupling percentages particularly at low temperature regions and the difficulties in sample weighing due to moisture condensation on the surface of the sample during sample loading.

2. Calculation of Magnetization Values

To quantify the entrapped O_2 molecules in both the THF+O_2 and O_2 clathrate hydrates, we performed direct release measurements by dissociating the clathrate hydrate samples in a water bath (Table 1). For reliable reproducibility, the experiment was repeated five times. In combination with the ideal gas law and previous

Table 1. Direct release measurements of the THF+O_2 and O_2 hydrates at 288 K and atmospheric pressure

	THF+O_2 hydrate	O_2 hydrate
Released O_2 (ml/g H_2O)	62 (±5)	175 (±10)

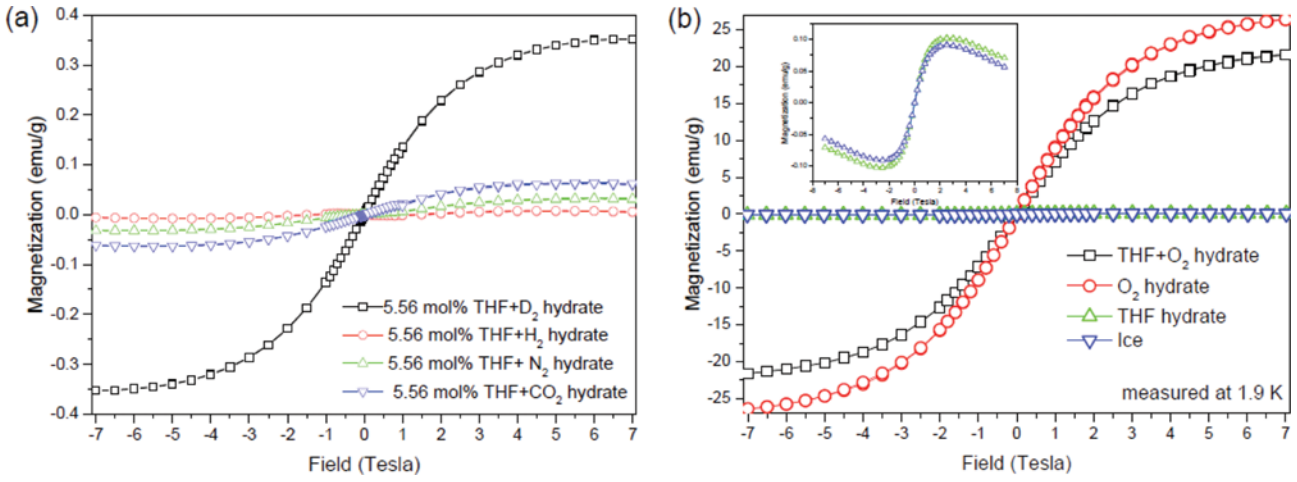

Fig. 2. Isothermal magnetic hysteresis loops *M*(*H*) of (a) various THF hydrates including H_2, D_2, N_2 and CO_2, and (b) hexagonal ice, THF hydrate, THF+O_2 hydrate and O_2 hydrate measured at 1.9 K.

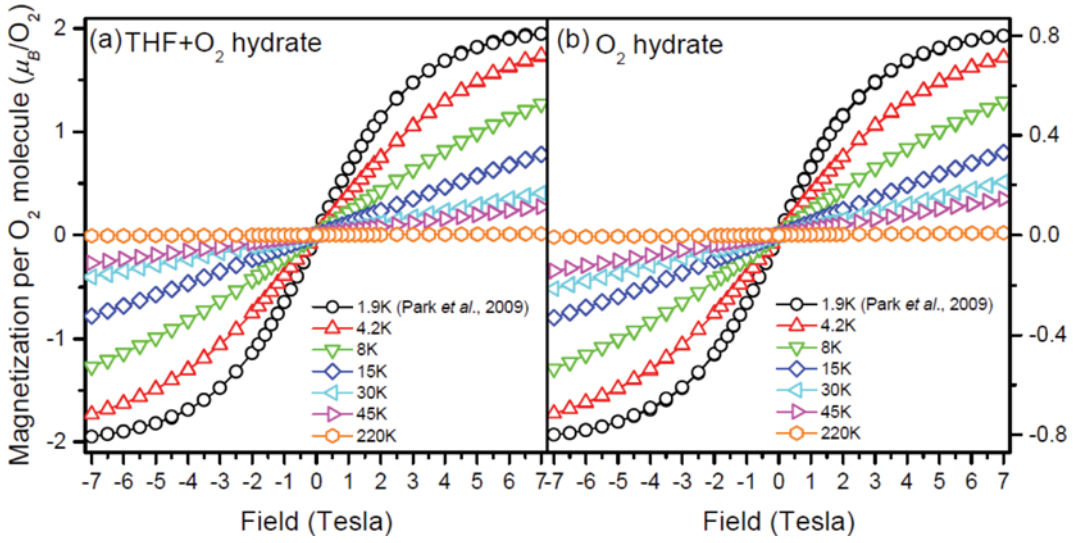

Fig. 3. Isothermal magnetic hysteresis loops *M*(*H*). The *M*(*H*) of (a) THF+O_2 hydrate and (b) pure O_2 hydrate as a function of temperature.

neutron diffraction analysis results [6], the THF+O_2 hydrate contained approximately 6.4 O_2 molecules per 136 H_2O. On the other hand, O_2 hydrate has approximately 20.8 O_2 molecules per 136 H_2O with an additional 15 wt% of hexagonal ice. To evaluate the magnetization per O_2 for both the THF+O_2 and O_2 hydrates, the cage occupancies (for the THF+O_2 hydrate, $\theta_{S,O_2}\approx0.4$; for O_2 hydrate, $\theta_{S,O_2}\approx0.8$ and $\theta_{L,O_2}\approx1$) from previous neutron diffraction results were used [6]. For the THF+O_2 hydrate, the total mass (guest+host) per unit cell (u.c) is 3228.8 g/u.c. In the case of the O_2 hydrate, the total mass (guest+host with unreacted ice phase (15 wt%)) is 3013.8 g/u.c. For example, at 7 Tesla and 1.9 K, the magnetization values per mass for the THF+O_2 and O_2 hydrates are 21.6 and 26.5 emu/g, respectively (Fig. 2(b)). Thus, the magnetization value per unit cell for the THF+O_2 and O_2 hydrates at 7 Tesla and 1.9 K are 69742.1 emu/u.c. (=21.6 emu/g×3228.8 g/u.c.) and 79865.7 emu/u.c. (=26.5 emu/g×3013.8 g/u.c.), respectively. With the basis of the number of O_2 molecules contained in the unit cell the THF+O_2 and O_2 hydrates were determined to have magnetization values of 10897.2 emu/O_2 (1.95 μ_B/O_2) and 4517.3 emu/O_2 (0.81 μ_B/O_2), respectively. The magnetization values of the THF+O_2 and O_2 clathrate hydrates at various temperature ranges (1.9-220 K) were also determined in the same way, and the results are shown in Fig. 3.

RESULTS AND DISCUSSION

To explore the magnetic properties of oxygen molecules forming a 3-d superstructure in the *sII* clathrate hydrate, direct current (dc) magnetic measurements using MPMS were performed. The magnetization values of various gas molecules in THF hydrates were measured and the results are shown in Fig. 2(a). Compared to the gas molecules shown in Fig. 2(a), the THF+O_2 and pure O_2 clathrate hydrates show significantly high magnetization values of 21.6 and 26.5 emu/g, respectively (Fig. 2(b)). The THF clathrate hydrate and host water-ice frameworks before inserting oxygen

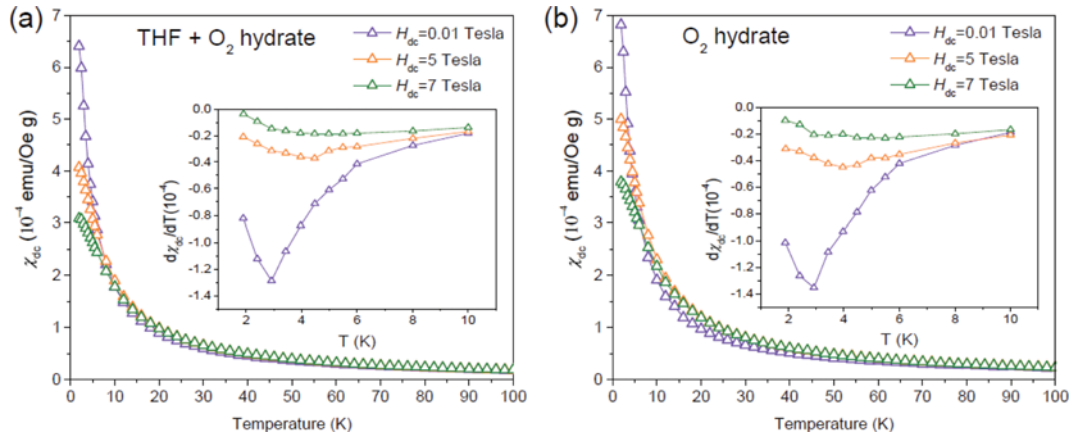

Fig. 4. Magnetic susceptibilities of THF+O_2 hydrate and pure O_2 hydrate as a function of temperature. The dc magnetic susceptibility of χ_{dc}(T) of (a) THF+O_2 hydrate and (b) O_2 hydrate in dc magnetic fields, where the insets show the corresponding differential magnetic susceptibility dχ_{dc}/dT vs. T curves.

molecules showed negligible magnetic behavior in comparison with the O_2 entrapped clathrate hydrate. Therefore, the following magnetic data are presumably due to the magnetic oxygen molecules entrapped in water-ice cages. Oxygen is a unique molecule showing a strong magnetic property in nature. The nonzero electronic spin number (S=1) of oxygen molecules in the ground electron state $3\Sigma_g^-$ induces oxygen molecules to have a magnetic property [15]. Oxygen molecules of a gaseous phase exhibit paramagnetic behavior, while solid oxygen at a low temperature shows antiferromagnetic behavior for all three crystallographic phases of α, β, and γ associated with structural characteristics of the molecular crystal. Confinement of magnetic oxygen molecules into a porous nanostructure and the concomitant formation of low dimensional superstructures, such as two-dimensional (2-d) antiferromagnetic oxygens filled in graphite and one-dimensional (1-d) oxygen dimers adsorbed in metal-organic solids, modify its physical properties [16-19]. Contrary to a typical antiferromagnetic property of solid oxygen, it is noticeable that the O_2-O_2 pair with the crossed X-structure can possess a ferromagnetic property theoretically [20].

To clearly see the differences in magnetic properties between THF+O_2 and pure O_2 clathrate hydrates, isothermal magnetic hysteresis loops $M(H)$ were measured at various temperature conditions. A previous report revealed that the field-dependent magnetization patterns of THF+O_2 hydrate (1.95 μ_B/O_2) significantly differed from that of the pure O_2 hydrate (0.81 μ_B/O_2) at 1.9 K and 7 Tesla, where saturated magnetization was observed [6]. The surprising feature was that even though the number of entrapped magnetic oxygen molecules is much larger in the pure O_2 clathrate hydrate ($20.8O_2 \cdot 136H_2O$) than in the THF+O_2 clathrate hydrate ($6.4O_2 \cdot 136H_2O$), the magnetization value of the former is much smaller than that of the latter. A similar trend was also found at higher temperature conditions than 1.9 K (Fig. 3). A neutron powder diffraction analysis in the previous study revealed that the nearest *sII-S* to *sII-L* distance of 6.04 Å on average, and the THF+O_2 hydrate was also confirmed to have a relatively low O_2 population value of 0.4 in the spatial distribution of magnetic guests, which is strongly influenced by the non-magnetic guests (THF) already positioned in *sII-L*. Thus, the distance between two neighboring O_2 molecules entrapped in *sII-S* is believed to be much further apart than 6.04 Å, implying that its unique magnetic property has a strong relationship with weakly interacting O_2 molecules. Accordingly, the higher magnetization value for the THF+O_2 hydrate might be due to the field-induced 'ferromagnetic-like' order of the magnetic moment of O_2 molecules. Significantly, this implies that the encaged O_2 exhibits behavior similar to a pseudo-isolated molecule, nearly following the behavior of a pure O_2 spin state which has a theoretical saturation value of 2.0 μ_B/O_2 [7].

Fig. 4 displays a temperature dependence of dc magnetic susceptibility χ_{dc}(T) for the THF+O_2 and pure O_2 clathrate hydrates. The observed magnetic properties of both the THF+O_2 and pure O_2 clathrate hydrates are largely different from the well-known antiferromagnetic properties of solid oxygen and the entrapped O_2 in previous reports [15-19,21,22]. The χ_{dc}(T) curves exhibit paramagnetic-like behavior over a broad temperature range. Compared to typical paramagnets, however, slightly different features are found at low temperature region. As the temperature decreases, the magnetic susceptibility χ_{dc}(T) continuously increases. In particular, as the external magnetic field decreases, χ_{dc}(T) increases at low temperature condition approximately below 10 K. As the external magnetic field increases, remarkably, the slope of χ_{dc}(T) is slightly blunted at around 4 K. We plotted the differential dc magnetic susceptibility dχ_{dc}(T)/dT in the insets of Figs. 4(a) and 4(b) to clearly see this slope change. The minimum point of the dχ_{dc}(T)/dT curve was observed at around 3 K in 0.01 Tesla, and it was shifted to a slightly higher temperature of about 5.5 K in 7 Tesla. As reported in previous study, the magnetic property of oxygen molecules was largely affected by a thermal fluctuation at a zero field [6], and as a result the magnetic moments of oxygen molecules tend to be aligned randomly. In a high external magnetic field of about 7 Tesla, however, the slope change in dχ_{dc}(T)/dT at around 4 K suggests a field-induced alignment of the oxygen magnetic moments.

As seen above, the THF+O_2 and pure O_2 clathrate hydrates exhibit a difference in the field-induced saturated moment, but their χ_{dc}(T) curves seem to have similar features. To investigate the characteristics of the field-induced alignments of the oxygen magnetic moments, we analyzed the inverse dc magnetic susceptibility 1/χ_{dc}(T)

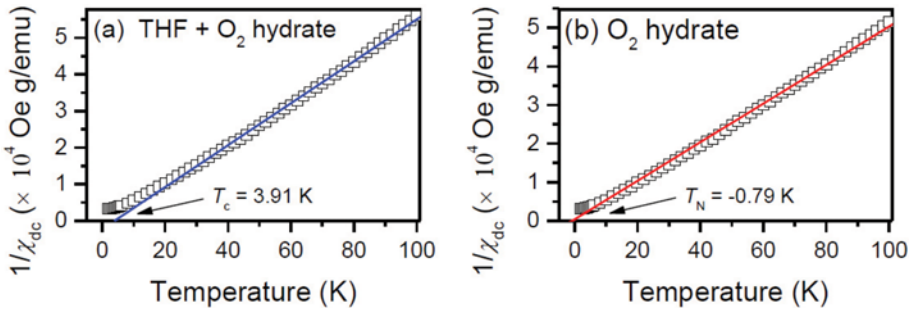

Fig. 5. Temperature dependence of the inverse magnetic susceptibility. $1/\chi_{dc}$(T) curve of (a) THF+O_2 hydrate and (b) O_2 hydrate measured at H_{dc}=7 Tesla. The solid lines are the Curie-Weiss fits to measured data (symbol) in the temperature range of 20-100 K.

using the Curie-Weiss law. Fig. 5 shows the inverse dc magnetic susceptibility $1/\chi_{dc}$(T) with the temperature for the THF+O_2 and pure O_2 clathrate hydrates measured at H_{dc}=7 Tesla. The $1/\chi_{dc}$(T) curves are slightly bent with the change of temperature, and consequently the measured data (symbols) for the whole temperature range are not well fitted by a linear function of Curie-Weiss law. We selected the measured data in a range of 20-100 K, at which the data should be independent of a field-induced non-linear behavior of $1/\chi_{dc}$(T) typically observed in a low temperature region, and performed a fitting to the Curie-Weiss law (solid lines). The $1/\chi_{dc}$(T) curve for the binary THF+O_2 clathrate hydrate shows an upward deviation from the linear curve at a low temperature region, while the pure O_2 clathrate hydrate displays a tendency of less upward deviation than the binary THF+O_2 clathrate hydrate. From the fittings to the Curie-Weiss law $1/\chi_{dc} \propto (T - T_{C,N})$, we found that the binary THF+O_2 clathrate hydrate has a ferromagnetic-like feature of positive Curie temperature T_C (Curie temperature)=+3.91 K, as shown in Fig. 5(a). On the other hand, the pure O_2 clathrate hydrate reveals an antiferromagnetic-like feature with a negative temperature intercept, *i.e.*, T_N (Neél temperature)=−0.79 K (Fig. 5(b)).

Heat capacity measurements of THF+O_2 and O_2 clathrate hydrates at low temperatures are of interest because the measurements possibly allow an estimation of the magnetic entropy, in particular, zero-point entropy associated with geometrical frustration inherent in the structure [23]. Fig. 6(top) exhibits specific heat capacities of THF+O_2 and pure O_2 hydrates as a function of temperature. As the temperature decreases, the heat capacity continuously decreases. However, the decreasing tendencies at low temperature regions in both the THF+O_2 and pure O_2 hydrates seem to differ significantly from the patterns at approximately above 5 K. To

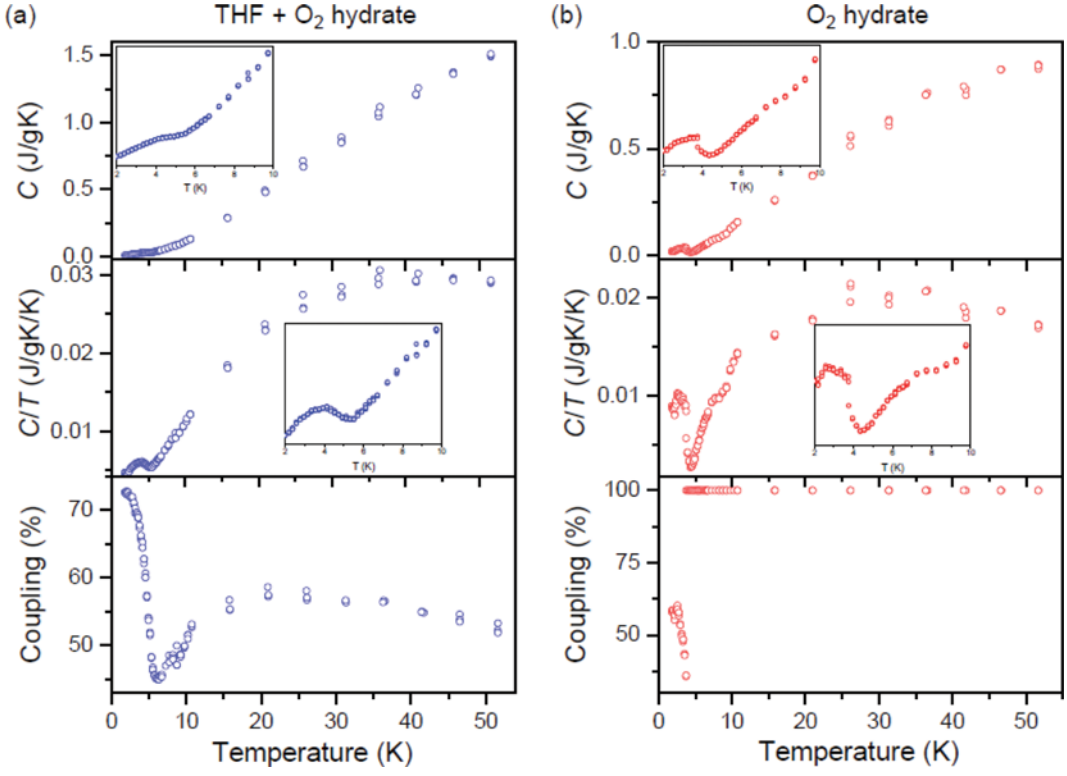

Fig. 6. Heat capacity measurements of (a) THF+O_2 hydrate and (b) O_2 hydrate in the temperature range of 1.8-50 K.

clearly identify the transition behavior, C/T values were plotted as shown in the middle of Fig. 6. The transitions of the heat capacity observed at approximately below 5 K are conjectured to the Curie or Neél temperatures for THF+O_2 or pure O_2 clathrate hydrates, respectively. In these experiments, we were able to observe the peak behavior at low temperature only qualitatively, but the results appear to be not sufficient for a quantitative analysis because of the weak thermal coupling between sample and sample holder (Fig. 6(bottom)) inherently occurring in the highly sensitive icy materials used in the present study. Future studies include the investigation of a quantitative analysis of the transition patterns in the heat capacity.

CONCLUSIONS

Binary THF+O_2 and pure O_2 clathrate hydrates, which were prepared by a selective injection of guest molecules into water-ice cages, display a clear difference in the magnetic properties associated with the 3-d superstructure of the guest magnetic oxygens. We expect that this work will draw considerable attention from researchers involved in inclusion chemistry and related engineering to create new functional complex materials.

ACKNOWLEDGEMENTS

This research was supported by Basic Science Research Program through the National Research Foundation of Korea (NRF) funded by the Ministry of Education (NRF-2015R1D1A1A02061741).

REFERENCES

1. L. Pauling and R. E. Marsh, *Proc. Natl. Acad. Sci. U.S.A.*, **38**, 112 (1952).
2. J. L. Atwood, J. E. D. Davies and D. D. MacNicol, Inclusion Compounds, Vol. 1, Academic Press Inc., London (1984).
3. E. D. Sloan and C. Koh, Clathrate Hydrates of Natural Gases, CRC Press, New York, 3rd Ed. (2007).
4. H. Lee, J.-w. Lee, D. Y. Kim, J. Park, Y.-T. Seo, H. Zeng, I. L. Moudrakovski, C. I. Ratcliffe and J. A. Ripmeester, *Nature*, **434**, 743 (2005).
5. Y. Park, D.-Y. Kim, J.-w. Lee, D.-G. Huh, K.-P. Park, J. Lee and H. Lee, *Proc. Natl. Acad. Sci. U.S.A.*, **103**, 12690 (2006).
6. Y. Park, J. Dho, J. Seol, S.-H. Yeon, M. Cha, Y. H. Jeong, Y. Seo and H. Lee, *J. Am. Chem. Soc.*, **131**, 5736 (2009).
7. S. T. Bramwell and M. J. P. Gingras, *Science*, **294**, 1495 (2001).
8. L. Pauling, *J. Am. Chem. Soc.*, **57**, 2680 (1935).
9. J. Snyder, J. S. Slusky, R. J. Cava and P. Shiffer, *Nature*, **413**, 48 (2001).
10. R. F. Wang, C. Nisoli, R. S. Freitas, J. Li, W. McConville, B. J. Cooley, M. S. Lund, N. Samarth, C. Leighton, V. H. Crespi and P. Schiffer, *Nature*, **439**, 303 (2006).
11. K. H. Fischer and J. A. Hertz, Spin glasses, Cambridge University Press (1993).
12. M. J. Harris, S. T. Bramwell, D. F. McMorrow, T. Zeiske and K. W. Godfrey, *Phys. Rev. Lett.*, **79**, 2554 (1997).
13. C. Bansal, H. Kawanaka, H. Bando and Y. Nishihara, *Phys. Rev. B*, **66**, 052406 (2002).
14. M. J. P. Gingras, B. C. den Hertog, M. Faucher, J. S. Gardner, S. R. Dunsinger, L. J. Chang, B. D. Gaulin, N. P. Raju and J. E. Greedan, *Phys. Rev. B*, **62**, 6496 (2000).
15. Y. A. Freiman and J. J. Jodi, *Phys. Rep.*, **401**, 1 (2004).
16. R. Kitaura, S. Kitagawa, Y. Kubota, T. C. Kobayashi, K. Kindo, Y. Mita, A. Matsuo, M. Kobayashi, H.-C. Chang, T. C. Ozawa, M. Suzuki, M. Sakata and M. Takata, *Science*, **298**, 2358 (2002).
17. A. Oda, T. Kawakami, S. Takeda, W. Mori, M. M. Matsushita, A. Izuoka, T. Sugawara and K. Yamaguchi, *Mol. Cryst. Liq. Cryst.*, **306**, 151 (1997).
18. T. C. Kobayashi, A. Matsuo, M. Suzuki, K. Kondo, R. Kitaura, R. Matsuda and S. Kitagawa, *Prog. Theore. Phys. Suppl.*, **159**, 271 (2005).
19. S. Takamizawa, E. Nakata and T. Akatsuka, *Angew. Chem. Int. Ed.*, **45**, 2216 (2006).
20. B. Bussery and P. E. S. Wormer, *J. Chem. Phys.*, **99**, 1230 (1993).
21. D. F. Evans and R. E. Richards, *Nature*, **169**, 246 (1952).
22. U. Köbler and R. Marx, *Phys. Rev. B*, **35**, 9809 (1897).
23. A. P. Ramirez, A. Hayashi, R. J. Cava, R. Siddharthan and B. S. Shastry, *Nature*, **399**, 333 (1999).